THE JOURNAL OF PHYSICAL CHEMISTRY A

Article

pubs.acs.org/JPCA

Oxyhalogen−Sulfur Chemistry: Kinetics and Mechanism of Oxidation of Chemoprotectant, Sodium 2-Mercaptoethanesulfonate, MESNA, by Acidic Bromate and Aqueous Bromine

Risikat Ajibola Adigun,[†] Morgen Mhike,[†] Wilbes Mbiya,[†] Sreekanth B. Jonnalagadda,[†,‡] and Reuben H. Simoyi[†,‡,*]

[†]Department of Chemistry, Portland State University, Portland, Oregon 97207-0751, United States

[‡]School of Chemistry and Physics, University of KwaZulu-Natal, Westville Campus, Durban 4000, South Africa

ABSTRACT: The oxidation of a well-known chemoprotectant in anticancer therapies, sodium 2-mercaptoethanesulfonate, MESNA, by acidic bromate and aqueous bromine was studied in acidic medium. Stoichiometry of the reaction is: $BrO_3^- + HSCH_2CH_2SO_3H \rightarrow Br^- + HO_3SCH_2CH_2SO_3H$. In excess bromate conditions the stoichiometry was deduced to be: $6BrO_3^- + 5HSCH_2CH_2SO_3H + 6H^+ \rightarrow 3Br_2 + 5HO_3SCH_2CH_2SO_3H + 3H_2O$. The direct reaction of bromine and MESNA gave a stoichiometric ratio of 3:1: $3Br_2 + HSCH_2CH_2SO_3H + 3H_2O \rightarrow HO_3SCH_2CH_2SO_3H + 6Br^- + 6H^+$. This direct reaction is very fast; within limits of the mixing time of the stopped-flow spectrophotometer and with a bimolecular rate constant of $1.95 \pm 0.05 \times 10^4\ M^{-1}\ s^{-1}$. Despite the strong oxidizing agents utilized, there is no cleavage of the C−S bond and no sulfate production was detected. The ESI−MS data show that the reaction proceeds via a predominantly nonradical pathway of three consecutive 2-electron transfers on the sulfur center to obtain the product 1,2-ethanedisulfonic acid, a well-known medium for the delivery of psychotic drugs. Thiyl radicals were detected but the absence of autocatalytic kinetics indicated that the radical pathway was a minor oxidation route. ESI−MS data showed that the *S*-oxide, contrary to known behavior of organosulfur compounds, is much more stable than the sulfinic acid. In conditions where the oxidizing equivalents are limited to a 4-electron transfer to only the sulfinic acid, the products obtained are a mixture of the *S*-oxide and the sulfonic acid with negligible amounts of the sulfinic acid. It appears the *S*-oxide is the preferred conformation over the sulfenic acid since no sulfenic acids have ever been stabilized without bulky substituent groups. The overall reaction scheme could be described and modeled by a minimal network of 18 reactions in which the major oxidants are HOBr and $Br_2(aq)$.

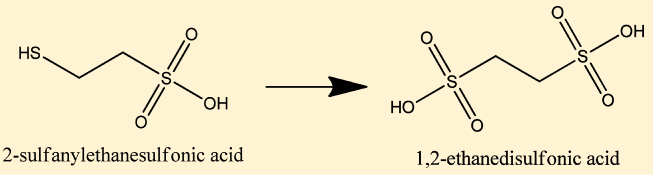

INTRODUCTION

Renal failure in cancer patients is a common problem in oncology. This complication is frequently multifactorial in origin.[1] Several antineoplastic agents are potentially nephrotoxic. Pre-existing renal impairment, combined with administration of potentially nephrotoxic drugs increase the risk of nephrotoxicity.[2−4] Methotrexate-related renal damage most frequently occurs with high-dose therapy and can be avoided by forced alkaline diuresis and administration of folinic acid.[4] Cisplatin nephrotoxicity is dose-related and, in the absence of a chemoprotectant (an agent which provides protection against toxic effects of a chemotherapy agent), used to be considered dose-limiting.[5] These drugs form an integral part of chemotherapy regimens used in cancer treatment. For instance, cisplatin is used in 50−70% of all cancer patients most often in combination with other drug(s).[6] Most anticancer drugs and their metabolites are eliminated through the kidneys, thus, making the kidneys susceptible to injury.[7]

Sodium 2-mercaptoethanesulfonate, MESNA (trade name Mesnex),[8] is a low molecular weight thiol used clinically as a chemoprotectant to inhibit anticancer drug-induced neurotoxicity, nephrotoxicity, hemorrhagic cystisis, myelo-suppression, and urothelial toxicity. MESNA has also been found to prevent contrast medium-induced nephropathy, a common complication in radiographic procedures.[8] Its clinical development and subsequent application as a chemoprotectant was triggered by the dose-limiting nephrotoxicity associated with most antineoplastic drugs which make their administration in clinically effective doses impossible.[9−11] MESNA is of particular interest because it ameliorates associated toxicity without reducing efficacy of the administered anticancer drug.[12−14] Successful phase II clinical trials have already been undertaken on the prophylactic use of Mesnex for women receiving a regimen of carboplatin and ifosfamide for advanced breast cancer carcinomas.[14] This use of MESNA has been without a full analysis of its interactions with biological proteins or its possible bioactivation. Bioactivation and analysis of subsequent metabolites is necessary for the derivation of better nephroprotectant analogues.

Sulfur compounds undergo a variety of metabolic reactions, namely: oxidations, reductions, hydrolysis, and conjugations.[15]

Received: December 1, 2013
Revised: February 5, 2014
Published: February 7, 2014

Sulfur in most organic configurations is nucleophilic, and nucleophilic atoms are usually susceptible to metabolic activation via oxidation.[16] Thus, the oxidation of sulfur-containing compounds represents an important aspect of sulfur metabolism. These oxidations appear to be involved in many cellular functions, including the reductive degradation of polypeptide hormones and proteins, regulation of protein synthesis, maintenance of intracellular redox potential, and protection of the cell from oxidative damage.[17] Biological oxidations of organosulfur compounds are predominantly through S-oxygenation, in which there is successive addition of oxygen onto the sulfur center until it is oxidatively saturated to the +6 oxidation state.[18] The molecular basis for S-oxygenation of sulfur compounds is not well understood since relatively few studies have addressed this problem. Although S-oxygenation of xenobiotics by microsomes supplemented with NADPH and oxygen has been demonstrated repeatedly, the facile oxidations of sulfur compounds by hydrogen peroxide and other species of reduced oxygen, such as superoxide ion, frequently complicate interpretation of *in vitro* studies.[16] In general, the metabolism of chemically stable compounds depends on enzyme catalysis, and both the microsomal cytochrome P-450 system and the flavin-containing monooxygenases[19] are often implicated in S-oxygenations catalyzed by microsomes.

There are several biological oxidants in the physiological environment that are capable of oxidatively bioactivating thiol-based xenobiotics such as MESNA. These include molecular oxygen and reduced oxygen species such as superoxide anion radical, hydrogen peroxide and the hydroxyl radical. Other oxidants of importance are oxyhalogens HOCl and HOBr and molecular iodine, I_2. Stimulated granulocytes produce oxidizing agents (e.g., H_2O_2) and secrete granular proteins into the extracellular medium which contributes to their antimicrobial, cytotoxic and cytolytic activities.[20] Each group of cells contains a specific peroxidase which catalyzes the reactions of hydrogen peroxide with halogens. The enzyme *myeloperoxidase* which is abundant in neutrophils catalyzes the oxidation of Cl^- ions by H_2O_2 to yield HOCl:[21]

$$H_2O_2 + Cl^-/Br^- + \text{myeloperoxidase}/H^+ \rightarrow HOCl/HOBr + H_2O$$

HOCl and HOBr are capable of destroying a variety of microoganisms and mammalian cell targets.[22] They are also believed to be involved in the inflammatory response.[22] HOCl is, however, a short-lived oxidant. It has been demonstrated that HOCl generates longer-lived oxidizing species through its reaction with nitrogen compounds to yield chlorinated nitrogen derivatives with a N−Cl bond.[23] This might include the chlorinated derivatives with the α-amino acid taurine: $ClHNCH_2CH_2SO_3H$. The chloramine derivatives can thus continue to moderate the neutrophil toxicity long after HOCl has been depleted. Human bodies contain a very high concentration of Cl^- ions, nearly up to 0.1 M, and Br^- ions at 0.001 M. It is difficult to exclude HOCl and HOBr in any meaningful representation of possible oxidation reactions *in vivo*. It would appear plausible that HOCl and HOBr will react rapidly and efficiently with thiols, thiocarbamides, thioamides and thioethers before any reactivity might take place with inert amino acids such taurine. Though not a biological oxidant, precursor of HOBr is BrO_3^- and it is being used here as an oxidant because it generates the intermediate that is useful in following the reaction, with the exact mechanism of the HOBr and Br_2 oxidations being inferred from the overall reaction scheme.

Our research group has worked extensively on elucidating mechanisms of organosulfur reactions that are of direct relevance to metabolic activation of drugs and other xenobiotics with anticipation of better understanding of biological activities and insights into the course of events at the molecular level.[24] To this end, we present details of a kinetics and mechanistic study of interaction of MESNA with acidified bromate and aqueous bromine following observations from several studies in our laboratories indicating HOBr to be most significant oxidizing species involved in BrO_3^- oxidations with resultant production of bromine (another strong oxidizing species) in the presence of Br^-.[25−27] Use of nonphysiological conditions (low pH) is necessary since bromate is inert and pH 7.4. The use of such a strong oxidant system and in nonphysiological concentrations ensures that the oxidation of MESNA is complete in minutes, instead of the several hours it might take in the physiological environment. This also pushes the oxidation to the final oxidation products with no lingering intermediates which might complicate the kinetics. This manuscript focuses on the mechanism and detection of all possible metabolites in the oxidation of MESNA. Reaction kinetics were derived in conditions of equimolar to excess oxidant conditions to discourage sulfur's propensity of generating sulfur−sulfur polymerizations.

EXPERIMENTAL SECTION

Materials. Sodium bromate, perchloric acid (70−72%), sodium bromide, bromine, sodium thiosulfate, 5,5-dimethyl-1-pyroline-*N*-oxide (DMPO) (Fisher), barium chloride, sodium 2-mercaptoethanesulfonate, DCl, and D_2O (Sigma-Aldrich) were used without further purification. Bromine solutions, being volatile, were kept capped and standardized spectrophotometrically before each set of experiments. Water used for preparing reagent solutions was obtained from a Barnstead Sybron Corporation water purification unit capable of producing both distilled and deionized water (Nanopure).

Methods. Kinetics of MESNA−bromate and MESNA−bromine reactions were studied by monitoring the formation and consumption of bromine's isolated peak at 390 nm (ε = 142 $M^{-1}cm^{-1}$). All reactions were carried out at a constant temperature of 25 ± 0.5 °C and an ionic strength of 1.0 M using sodium perchlorate. Reactions between MESNA and bromate were monitored on a Perkin-Elmer Lambda 25 UV/vis spectrophotometer while bromine−MESNA reactions were studied using a Hi-Tech Scientific SF-61 stopped-flow spectrophotometer. Mass spectra of dynamic and product solutions were taken on a Thermo Scientific LTQ-Orbitrap Discovery mass spectrometer (San Jose, CA) equipped with electrospray ionization source operated in both the positive and negative modes.

Stoichiometric Determinations. For determination of excess oxidizing power at the end of a reaction, an iodometric titration method was used in which varying amounts of bromate were reacted with a fixed concentration of MESNA. Excess bromate concentrations were then evaluated by addition excess of acidified iodide and subsequent titration of the liberated iodine with standard sodium thiosulfate solution.

Product identification. For the bromate−MESNA reaction, Fourier Transform mass spectra (FTMS) of solutions containing stoichiometric amounts of bromate and MESNA were taken in the negative mode using electrospray ionization technique. Intermediates involved in the six-electron oxidation of MESNA by acidified bromate were observed and identified by recording mass spectra of the stepwise two-electron

dx.doi.org/10.1021/jp411790v | J. Phys. Chem. A 2014, 118, 2196−2208

oxidation of substrate by aqueous bromine. Products of reactions were further identified by nuclear magnetic resonance spectroscopy (NMR) using a Bruker Avance III (600-MHz ^{1}H) spectrometer and processed with Bruker Top Spin 2.1 software. Involvement of free radicals in the MESNA oxidations were evaluated on a Bruker Biospin e-scan spectrometer designed to perform electron paramagnetic resonance (EPR) measurements in the X-band-range.

RESULTS

Stoichiometry. Despite the use of a very strong oxidant, the sulfur center was not oxidized to sulfate, and remained tethered to the organic moiety to form a symmetric ethane disulfonic acid with a strictly 1:1 stoichiometry of bromate to MESNA:

$$BrO_3^- + HSCH_2CH_2SO_3H \rightarrow Br^- + HO_3SCH_2CH_2SO_3H \quad (R1)$$

The product; 1,2-ethanedisulfonic acid is a well-known medium for delivery of psychotic and hypnotic drugs such as chlomethiazole and prochlorperazine.[28] It is a very strong acid with pK_a values of −1.46 and −2.06. Results of the iodometric titration described in the experimental section above are shown in Figure 1. MESNA concentrations were held constant at

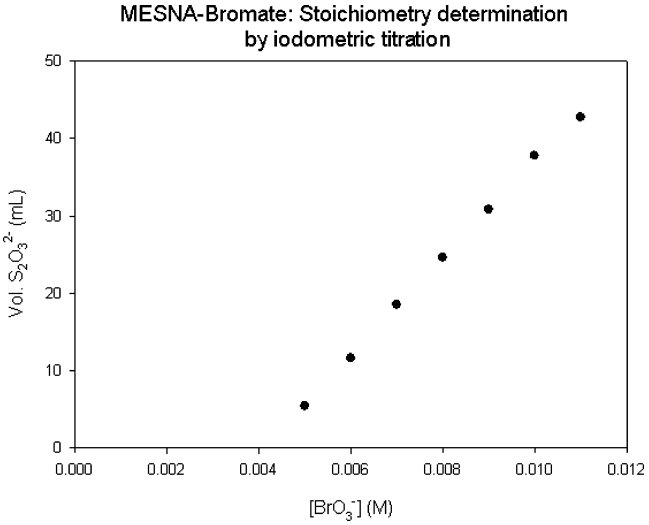

Figure 1. Plot used for the determination of the BrO_3^-−MESNA reaction. MESNA concentrations were constant at 4 mM while bromate concentrations were varied up to 11 mM. Solutions were incubated overnight and excess acidified iodide was added and liberated iodine titrated against standard thiosulfate with freshly prepared starch as indicator. The intercept, of 4 mM bromate, indicates complete depletion of bromate with no excess oxidizing power left in solution and represents the concentration of bromate needed to completely consume MESNA.

4 mM while bromate concentrations were varied from 5 mM to 11 mM. The thiosulfate titer was recorded for each variation of bromate and results plotted against the initial bromate concentrations. This gave a straight line of intercept (representing no excess oxidizing power left) at 4 mM bromate. Thus, a mixture of 4 mM each of MESNA and bromate, after complete reaction, afforded a product with no excess bromate concentrations to afford an iodometric titration. This was the stoichiometric ratio for the reaction R1. The reaction of aqueous bromine with MESNA was rapid enough such that the stoichiometry of the reaction was derived simply from titrating bromine (buret) into MESNA until the end point was attained from color observation. The experimentally determined stoichiometry for this reaction was 3:1:

$$3Br_2 + HSCH_2CH_2SO_3H + 3H_2O \rightarrow HO_3SCH_2CH_2SO_3H + 6Br^- + 6H^+ \quad (R2)$$

NMR Analysis. Figure 2a shows the normal NMR spectrum of MESNA in D_2O which shows the expected set of coupling triplets from the C−C backbone of MESNA. Each triplet integrated as two protons. A 1:1 mixture of bromate and MESNA in DCl shown in Figure 2b displays a single sharp NMR peak which appears downfield to both of the triplets in Figure 2a (ppm 3.19 vs 2.78 and 3.12 in Figure 2a). Figure 2c shows a 1:3 MESNA − bromine mixture NMR spectrum which also shows the expected single peak due to the methylene protons. The slight shift in the peak to ppm 3.16 is due to the fact that in Figure 2b, the solution was run in high acid, while in part c, the reaction was run in neutral conditions.

Reaction Kinetics. Formation of bromine was utilized to follow the reaction although bromine is not a product of the reaction being studied (stoichiometry R1). Bromine formation is a secondary reaction that involves excess bromate and the bromide formed in eq R1. Effectively, three reactions are proceeding simultaneously in any mixture of acidic bromate and MESNA: reactions R1, R2 and the BrO_3^-/Br^- reaction, reaction R3:

$$BrO_3^- + 5Br^- + 6H^+ \rightarrow 3Br_2 + 3H_2O \quad (R3)$$

Thus, in excess bromate conditions, the overall stoichiometry is a linear combination of reactions R1 and R3 which converts all the bromide from reaction R1 by oxidizing it to bromine:

$$6BrO_3^- + 5HSCH_2CH_2SO_3H + 6H^+ \rightarrow 3Br_2 + 5HO_3SCH_2CH_2SO_3H + 3H_2O \quad (R4)$$

From stoichiometry R4, amount of bromine formed is determined by initial MESNA concentrations. A spectrophotometric determination of final bromine concentrations in varying MESNA concentrations proved stoichiometry R4 of $0.60[MESNA]_0$. The direct bromine−MESNA reaction, reaction R2, was so much faster than either reactions R1 or R3 such that production of bromine is an indicator that the thiol is depleted. Thus, experimental observation of the reaction spectrophotometrically involved an initial quiescent period with no bromine formation. This induction period was then followed by a rapid bromine formation according to reaction R3. Time taken before bromine formation could then be related to rate of reaction R1.

Effect of Bromate. At constant acid and MESNA concentrations, bromate concentrations were varied at high excess over that needed for stoichiometry R1 ($[BrO_3^-]_0/[MESNA]_0 > 20$). Some of the experimental traces are shown in Figure 3a. There was a sharp end of the induction period and commencement of bromine formation was extremely rapid. The first 400 s are shown in Figure 3a. Expected bromine absorbance readings, based on stoichiometry R3 should be in the regions of 0.85. Thus, at 400 s, reaction R4 would not have gone to completion. At higher bromate concentrations (see trace d in Figure 3a), bromine concentrations show an initial transient peak which then gives way to the final bromine peak. Since reaction R3 is fast, transient bromine formation would

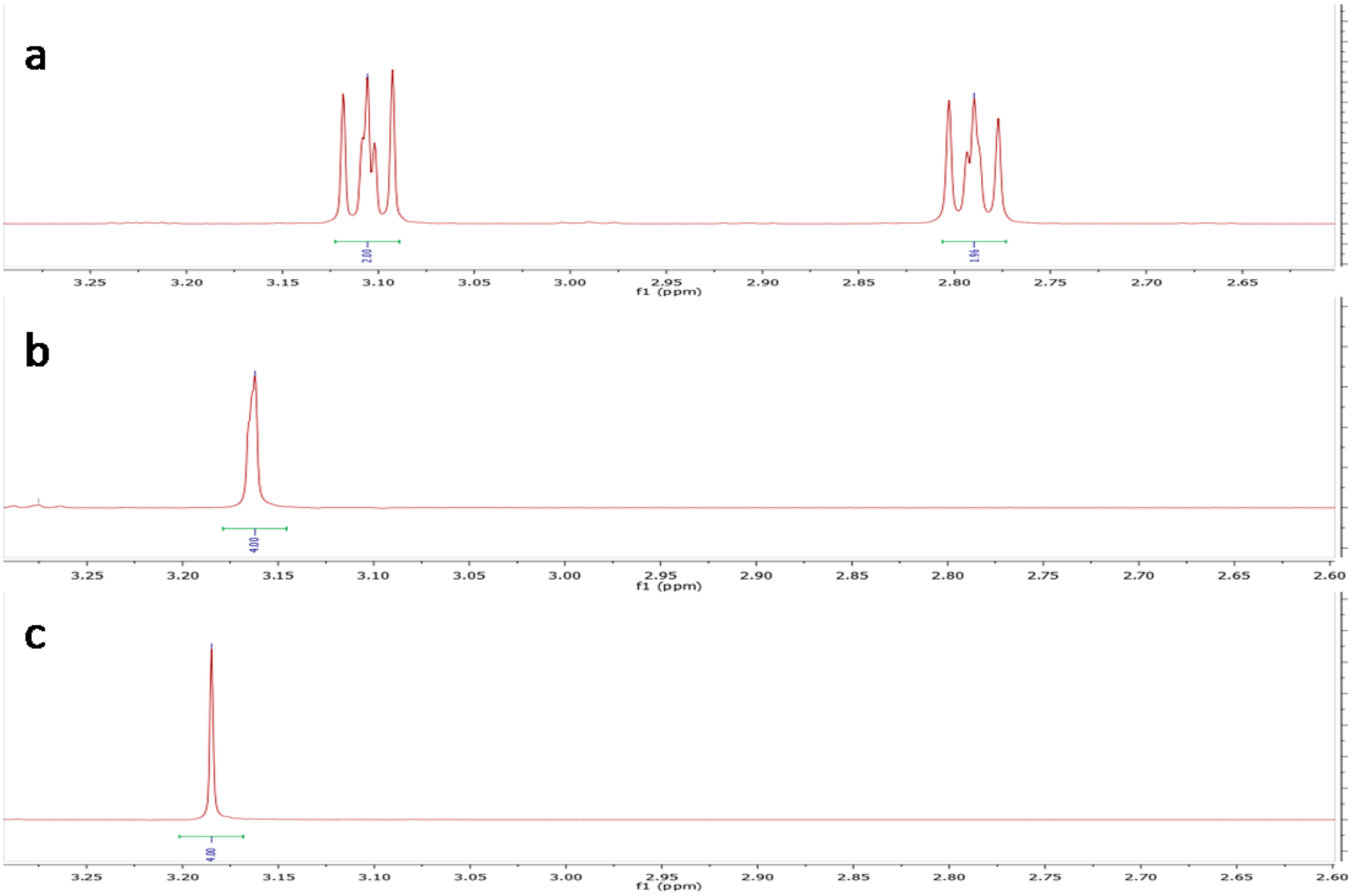

Figure 2. (a) Standard NMR spectrum of MESNA in D_2O. It shows the standard coupling triplets from the coupling sets of methylene protons with the protons adjacent to the sulfonic group being slightly more deshielded. (b) NMR spectrum of the final solution from a 1:1 mixture of bromate and MESNA in DCl. A solution with less than 1:1 bromate: MESNA gave a spectrum with both spectra (a and b). Only a single peak is observed as the two peaks from spectrum a coalesce and move slightly downfield as expected from the symmetric 1,2-ethylene disulfonic acid. (c) NMR spectrum from a 1:3 ratio of MESNA to bromine in D_2O. There is no trace of the original compound at these ratios with complete formation of the product.

suggest that one of the oxidation intermediates of MESNA is relatively stable. A plot of inverse of induction time vs $[BrO_3^-]_0$ shown in Figure 3b gives a straight line. This implies that the rate of the primary reaction of relevance to the point of bromine production is related to bromate concentrations to the first power. This would be the rate-determining step. The plot in Figure 3b also implicitly confirms stoichiometry R1. An induction period of infinity is when the inverse of the induction period is 0.00. This occurs when there is just enough bromate to oxidize MESNA completely with no excess bromate left to form bromine from the product of reaction R1, Br^-. With an initial concentration of 10 mM MESNA, the plot gives an intercept value of 10 mM bromate for reaction stoichiometry for reaction R1.

Effect of Acid. Acid is the most important catalyst in most oxyhalogen-based reactions.[29] It is also strongly catalytic in the bromate−MESNA reaction. Figure 4a shows that the induction period is rapidly shortened as acid concentrations are increased. The acid dependence of the induction period was an inverse square with saturation at high acid concentrations, tending toward simple inverse dependence (see Figure 4b). Low acid concentrations gave smooth bromine formation after the induction period, while high acid concentrations gave a hint of oligooscillatory behavior as that observed in Figure 3a.

Direct Br_2−MESNA Reaction. This reaction was extremely rapid, to the point of approaching the limits of the mixing time of the stopped-flow ensemble of 1 ms. Figure 5 shows some absorbance traces of the Br_2−MESNA reactions taken at varying initial MESNA concentrations. The reaction is essentially complete in 30 ms. The reaction showed first order dependence on both Br_2 and MESNA with a bimolecular rate constant of $1.95 \pm 0.05 \times 10^4$ M^{-1} s^{-1}.

MECHANISM

The general driving force for this reaction is controlled by the well-established oxyhalogen kinetics which involve a square dependence term in acid:[30−34]

$$H^+ + BrO_3^- \rightleftarrows HBrO_3 \quad \text{(R5)}$$

$$HBrO_3 + H^+ \rightleftarrows H_2BrO_3^+ \quad \text{(R6)}$$

$$H_2BrO_3^+ + 2e^- \rightarrow HBrO_2 + OH^- \quad \text{(R7)}$$

The oxidizing species is the protonated bromic acid. In standard oxyhalogen kinetics, the two electrons in reaction R7 are provided by Br^- which is oxidized to HOBr. Addition of bromide in conditions of excess bromate concentrations accelerated the rate of reaction and decreased the induction periods in Figures 3a and 4a. The resulting oxybromine species,

dx.doi.org/10.1021/jp411790v | J. Phys. Chem. A 2014, 118, 2196−2208

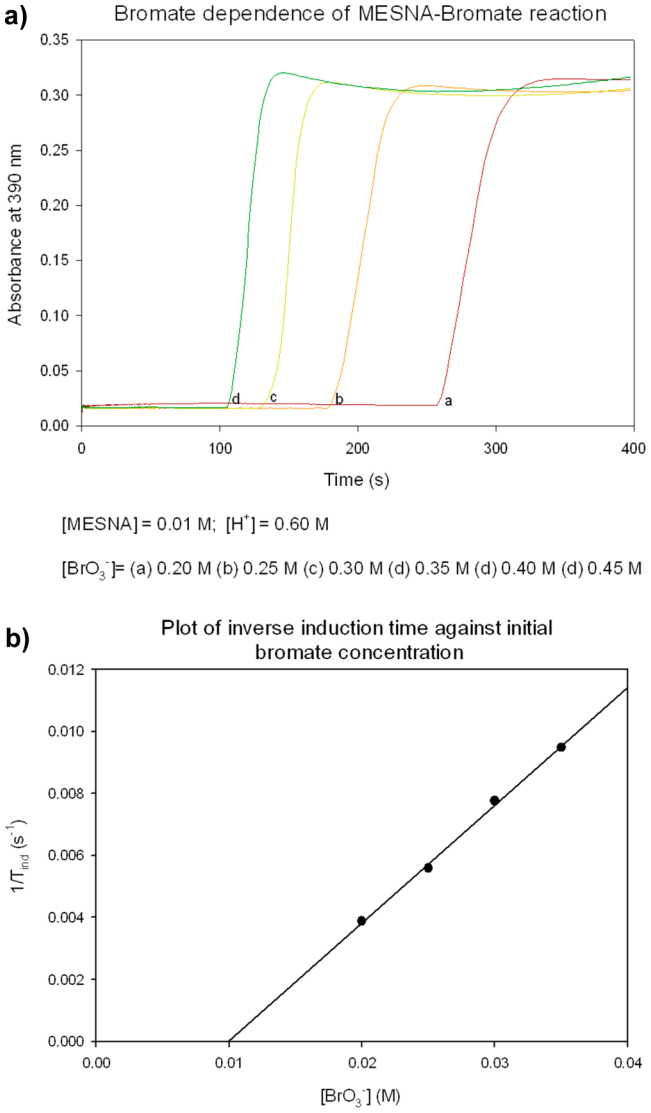

Figure 3. (a) Bromate dependence of the MESNA–bromate reaction. There is a rapid and sharp bromine formation after an induction period in which no bromine is formed. High bromate concentrations produce bromine so rapidly that it reaches an initial peak which gives way to a slower bromine formation until, in this case, the full bromine concentrations are attained at 6 mM (about 0.85 in absorbance). Ten mM $[MESNA]_0$; $[BrO_3^-]_0$ = (curve a) 0.20 M; (curve b) 0.25 M; (curve c) 0.30 M; (curve d) 0.35 M. (b) Plot of inverse of induction time vs initial bromate concentrations from the data shown in part a. Intercept represents induction time of infinity, which indicates that there is no excess bromate to form bromine; indicating the stoichiometric equivalent. This plot also confirms the 1:1 stoichiometry established from data in Figure 1.

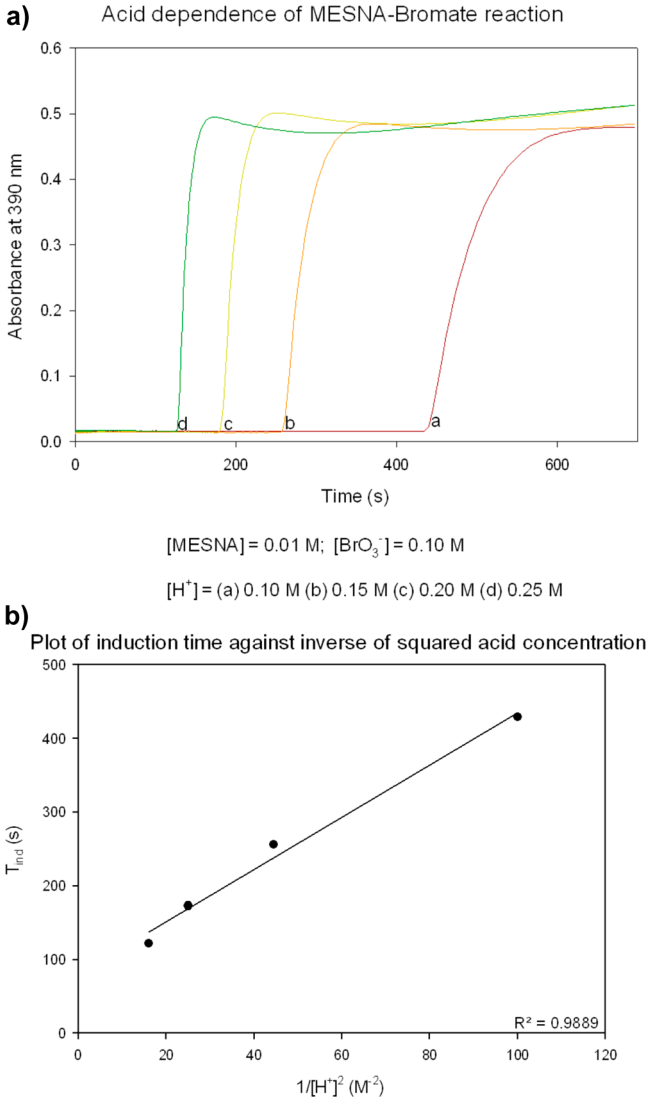

Figure 4. (a) Acid dependence of the bromate-MESNA reaction. Induction time decreases and rate of formation of bromine after induction period increases with acid. (b) No second order dependence could be discerned from the data in part a. Acid effect approaches first order in high acid, and second order for the slower low acid concentrations.

$HBrO_2$ and HOBr carry the bulk of the oxidation.[35] Since rate-determining step is reaction R7, the overall kinetics would be overall fourth order:

$$\text{rate} = k_0[BrO_3^-][H^+]^2[\text{Red}] \quad (1)$$

Red, the reductant, could be substrate MESNA or, initially, trace amounts of bromide in the reaction mixture always resident in any standard bromate solutions. Only catalytic amounts of bromide are needed in the R5–R8 cascade of reactions

$$H_2BrO_3^+ + Br^- \rightleftarrows HBrO_2 + HOBr \quad (R8)$$

$HBrO_2$ is known to be unstable with respect to HOBr in the presence of Br^-:[36]

$$HBrO_2 + Br^- + H^+ \rightleftarrows 2HOBr \quad (R9)$$

The major oxidant, if reaction R9 is labile in the forward direction, would be HOBr:

$$HOBr + H^+ + 2e^- \rightleftarrows Br^- + H_2O \quad (R10)$$

The initial part of this reaction system will be controlled by the sequence of reactions R5, R6, and R8–R10, if one utilizes the trace amounts of bromide in bromate solutions. The sum of these reactions shows that the overall stoichiometry of this initial part of the reaction is the conversion of two bromide ions to three bromide ions in the form of cubic autocatalysis:[37]

$$BrO_3^- + 6H^+ + 6e^- + 2Br^- \rightarrow 3Br^- + 3H_2O \quad (R11)$$

A slower direct reaction of bromate with substrate, MESNA, can also produce, initially, bromide, which can be used in reaction

dx.doi.org/10.1021/jp411790v | J. Phys. Chem. A 2014, 118, 2196–2208

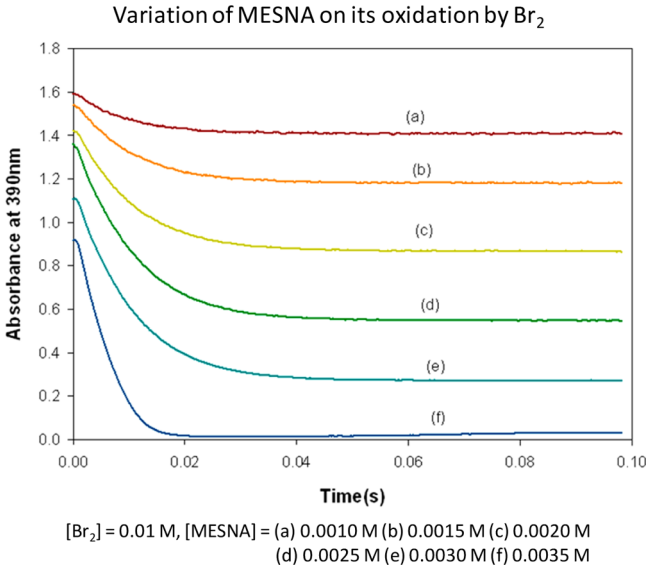

Figure 5. Direct reaction of bromine and MESNA. Variation of MESNA. The reaction is so fast it is close to the limits of our stopped-flow. The reaction is essentially over in 20 ms. The 3:1 stoichiometric ratio could also be graphically determined from the residual bromine absorbance. The reaction is strictly bimolecular.

R8 to produce the reactive oxidizing oxybromine species $HBrO_2$ and HOBr.

$$BrO_3^- + RSH + H^+ \rightarrow HBrO_2 + RSOH \quad (R12)$$

Reaction R12 can proceed with $HBrO_2$ as the oxidant to produce HOBr and Br^- in consecutive 2-electron transfers. Br^- can then catalyze the standard oxybromine kinetics which produce the active oxidizing species:[38,39]

$$BrO_3^- + 2H^+ + Br^- \rightleftarrows HBrO_2 + HOBr \quad (R13)$$

Reaction R13 is the accepted composite reaction R5 + R6 + R8 that explains second order acid kinetics in all bromate oxidations.[33]

Oxidation of MESNA. While the oxybromine kinetics are reasonably well-understood, not much is known on the thiol chemistry and sulfur oxidations in general. Thiol oxidations can proceed via a radical mechanism or through oxygen transfer.[40] The thiol group in MESNA is oxidized to the sulfonic acid, a 6-electron transfer. In general, a monotonic decrease in pH is observed when aqueous bromine is reacted with MESNA at neutral pH (stoichiometry R2) from the release of protons and final formation of the strong 1,2-ethanedisulfonic acid. The steady pH decrease suggests a sequential formation of the sulfur oxo-acids all the way to the formation of the sulfonic acid. It is reasonable to assume that the dominant pathway is via successive two-electron transitions from sulfur center in the −2 oxidation state to the +4 state in the sulfonic acid. A series of experiments were undertaken to prove this (Figure 6a−c). The first experiment involved the addition of an exactly 1:1 ratio of MESNA and aqueous bromine. This will be equivalent to a two-electron oxidation of the sulfur center. Sulfur, due to possible polymerizations, can attain several energetically accessible oxidation states, especially in conditions of excess reductant. Figure 6a shows an ESI−MS spectrum of the 1:1 MESNA − Br_2 reaction mixture after the reaction has been assumed to have gone to completion (these reactions have lifetimes of less than a second). The spectrum shows a strong peak for a product with an m/e value of 155.9560 which is equivalent to the addition of a single atom of oxygen to MESNA. It also shows a peak for the substrate, MESNA (m/e = 139.9610) and minor peaks for the dimeric MESNA and a MESNA plus two oxygen atoms adduct (m/e = 138.9534, 172.9585, respectively). Thus, three oxidation products are obtained with the dominant product being the one oxygen atom addition to MESNA. The form of this intermediate cannot be determined from ESI−MS data available. It could be the sulfenic acid, sulfoxide or the *S*-oxide. Sulfenic acids are very unstable and can only be stabilized by bulky substituent groups as in anthraquinones.[41,42] Sulfoxides can only be stabilized by a ring structure which can enhance the pi-bond stabilization. *Ab initio* calculations do not support a terminal sulfoxide without two electron-donating groups for stabilization.[43] Thus, the oxygen adduct appearing at m/e = 155.9562 should be an *S*-oxide (see structure **I** in Chart 1). Addition of two oxidizing equivalents (Figure 6b) does not produce predominantly, an adduct with two oxygen atoms, but still mostly the *S*-oxide and the sulfonic acid product (m/e = 188.9537). What would have been the sulfone or sulfinic acid ($HO_3SCH_2CH_2SO_2H$) appears to be unstable and disproportionates to the *S*-oxide and the sulfonic acid forms.

Known sulfinic acids derived from aminothiols are stabilized by resonance. Addition of the full 3 oxidizing equivalents the spectrum (Figure 6c) shows the dominant peak expected for the product 1,2-ethylene disulfonic acid (m/e = 188.9536) as well as its monosodium salt (m/e = 210.9356). No peak was observed for the disodium salt since bromine oxidations were conducted in neutral to slightly acidic pH. All the acid in this reaction solution was derived from the stoichiometry. Figure 6c shows no traces of the dimer nor the sulfinic acid, but does show small amounts of the *S*-oxide. We note, in parts a and b of Figure 6, before the addition of the 6-electron full oxidation equivalents that take the sulfur center to the sulfonic acid, peaks for the fully protonated dimeric MESNA at m/e = 280.924. The precursors for the dimeric species should either be a condensation-type reaction between an unoxidized thiol and the *S*-oxide; or thiyl radicals. The presence of the dimeric species and the series of oxygen-addition intermediates suggests at least two pathways for the oxidation of MESNA: successive 2-electron transfers from the sulfur center to the oxybromine center and a free radical-based initial oxidation pathway. A series of experiments were run using the X-band EPR spectrometer to detect any possible radical formation during the course of the reaction. Figure 7 shows the EPR spectra of the reaction solution using a DMPO trap. This shows the presence of an EPR-active adduct whose abundance increases with MESNA concentrations. All these reactions in excess bromate indicating that the radical species generated, mediated by MESNA, are derived from MESNA.

Radical Pathway and Its Significance. The mechanism of the generation of radicals from oxybromine chemistry is well-established. This pathway was derived from studies of the Belousov−Zhabotinskyi reaction, with the central species being the autocatalytic bromous acid.[35]

$$BrO_3^- + HBrO_2 + H^+ \rightleftarrows 2BrO_2^{\bullet} + H_2O \quad (R14)$$

$$BrO_2^{\bullet} + RSH \rightleftarrows RS^{\bullet} + HBrO_2 \quad (R15)$$

$$2RS^{\bullet} \rightarrow RSSR \quad (R16)$$

dx.doi.org/10.1021/jp411790v | J. Phys. Chem. A 2014, 118, 2196−2208

RSH is assumed to be the generic thiol, MESNA, and RSSR, the dimeric species at m/e = 280.9294. Reactions were not run in strictly anaerobic environments, and so the existence of the thiyl radicals can unleash a cascade of other radicals, specifically; superoxide, hydroxyl and hydrogen peroxide.[44] If one adds R14 + 2R15; and recognizing that the reaction is run in excess bromate, the overall stoichiometry shows that one $HBrO_2$ molecule will produce two $HBrO_2$molecules in quadratic autocatalysis. The autocatalytic production of bromous acid, coupled with its lability in reaction R9 should produce a constant enhancement of the reaction and deliver sigmoidal kinetics, which is typical for many bromate oxidations.[45] No autocatalysis was observed in this reaction and hence the radical pathway should not be the dominant route.

Effect of Acid. There was no observation of purely second order kinetics as expected from oxybromine kinetics.

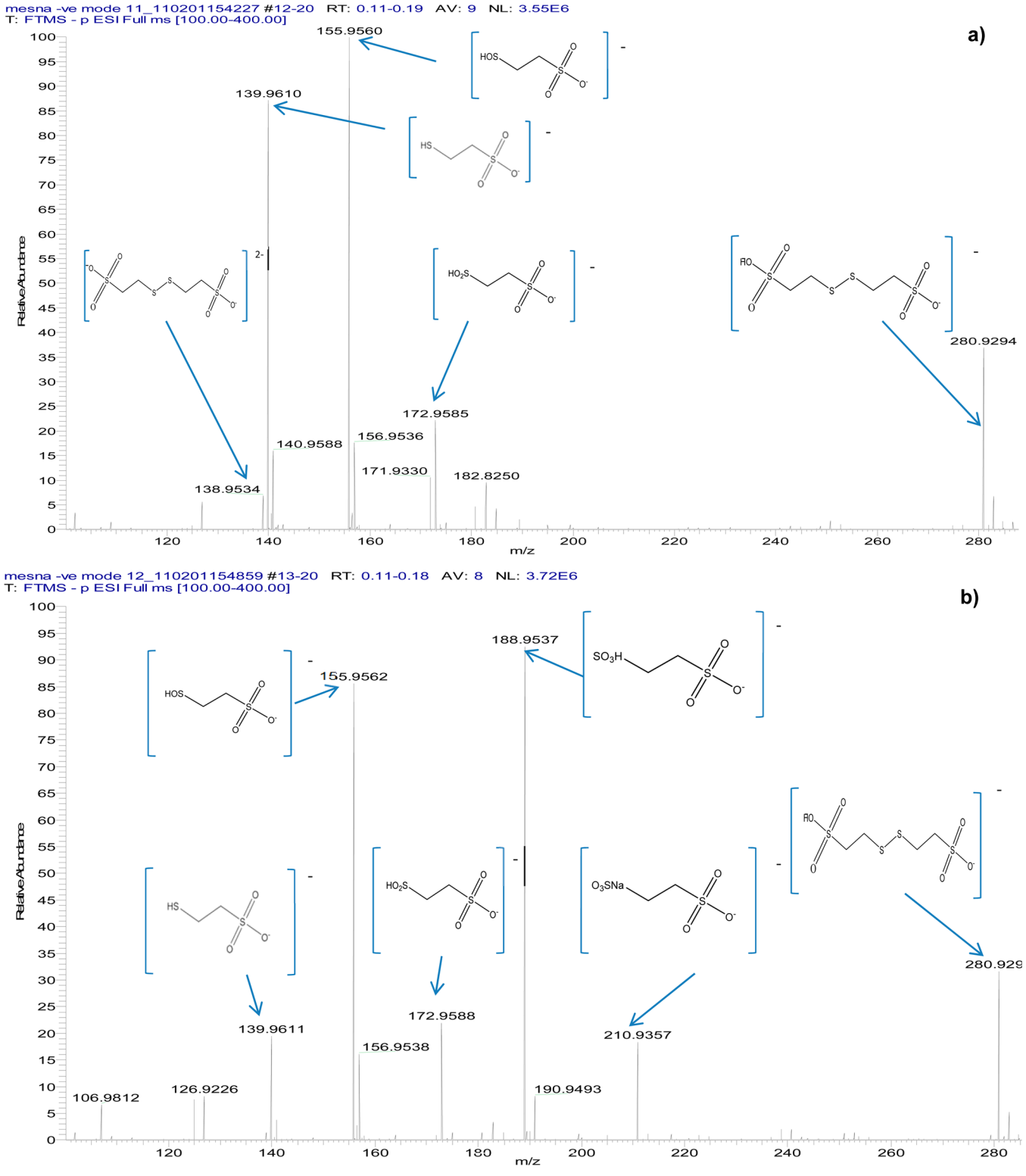

Figure 6. continued

dx.doi.org/10.1021/jp411790v | J. Phys. Chem. A 2014, 118, 2196−2208

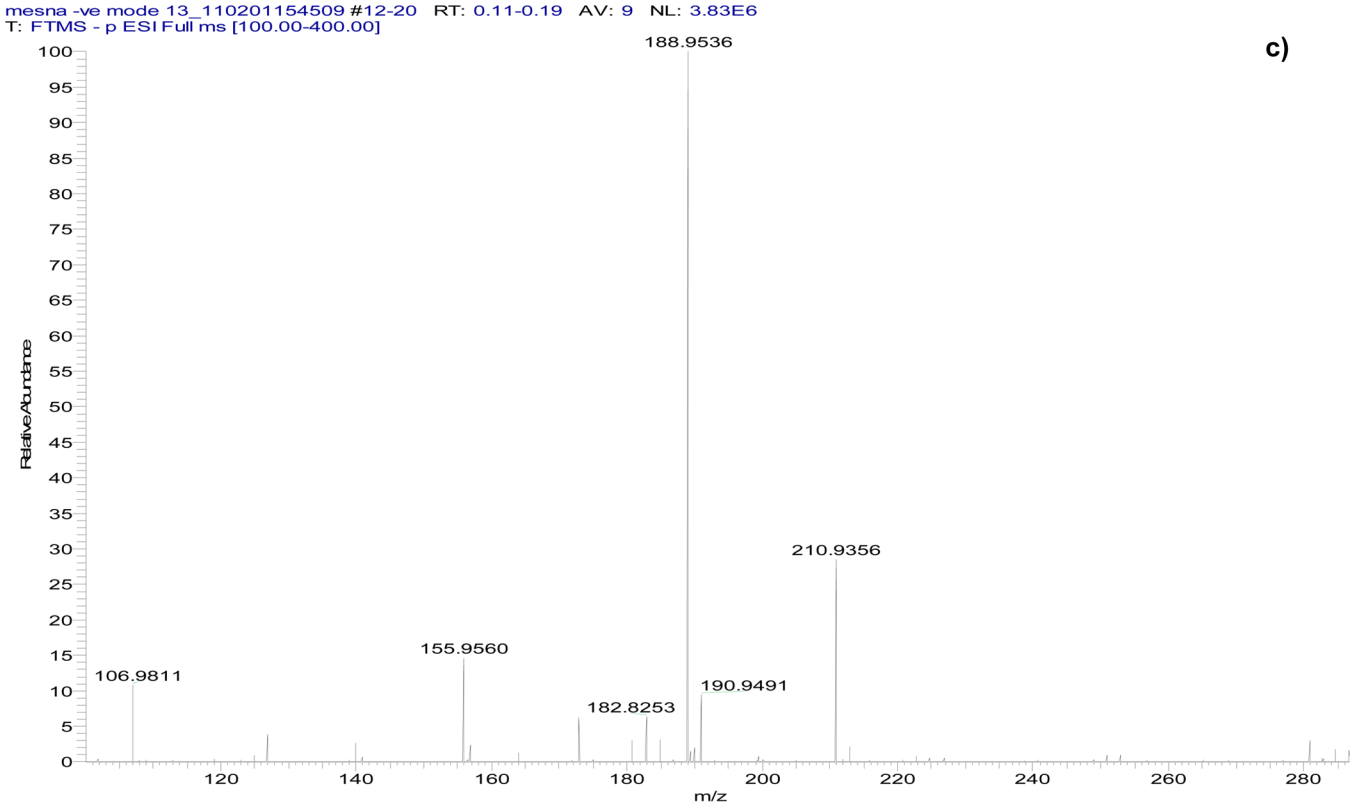

Figure 6. (a) ESI−MS spectrum of a reaction mixture of 1:1 MESNA−Br_2. The strongest peak is for the *S*-oxide at *m*/*e* 155.9560 apart from the substrate itself at 139.9610. Reaction is in slightly acidic medium, and thus shows both the protonated and unprotonated MESNA. A small peak for the dimeric species with an S −S bond can be seen at *m*/*e* 138.9534. There is a substantial peak for the singly charged dimeric species at 280.925. Some sulfinic acid can be seen at *m*/*e* 172.9585. This is essentially a mixture of metabolites in excess substrate which indicates that the *S*-oxide is the most stable intermediate at these conditions. (b) ESI−MS spectrum derived from addition of two equivalents of bromine. The sulfinic acid, which should be most abundant at these conditions, retains the same low abundance as in spectrum a; with the *S*-oxide and sulfonic acid being most abundant. The sulfinic acid (S(II)), if formed, rapidly disproportionates to the 0 and +4 oxidation states. The peak for MESNA has been reduced substantially from part a. (c) Addition of the full 3 equiv of bromine as according to the expected stoichiometry. MESNA peak disappears completely, living a large peak for the product, 1,2-ethylene disulfonic acid peak at *m*/*e* 188.9536 and a smaller peak for its monosodium salt at *m*/*e* 210.9356. There is no evidence of the sulfinic acid at these conditions; instead, a small and observable peak is still present for the *S*-oxide.

Chart 1. Structure I

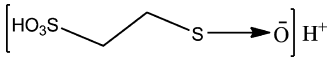

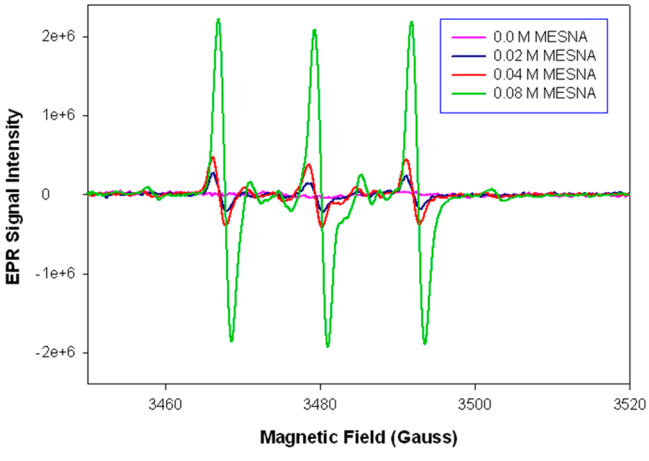

Figure 7. Formation of radicals, mediated by MESNA.

The complexity was derived from the thiol center, which is nucleophilic and would be protonated in highly acidic environments:

$$HO_3SCH_2CH_2SH + H^+ \rightarrow HO_3SCH_2CH_2SH_2^+, \quad K_b$$

If one considers the protonated thiol to be relatively inert, then the rate of reaction is

$$\text{rate} = \frac{k_0[BrO_3^-][H^+]^2[HO_3SCH_2CH_2SH]_T}{1 + K_b[H^+]}$$

where $[HO_3SCH_2CH_2SH]_T$ is the total of the protonated and unprotonated MESNA. Rate equation supports first order kinetics at high acid concentrations but expected second order kinetics at mild to low acid concentrations.

Overall Reaction Scheme. Both the oxidation product of MESNA and reduction product of bromate have been satisfactorily established. Contrary to most organosulfur compounds in the presence of a strong oxidant, the C−S bond does not cleave and no sulfate production is observed. The C−S bond is strengthened by the presence of electron-withdrawing groups on the carbon adjacent to the C−S bond.[46−49] Hence oxidation of cysteamine can only proceed as far as taurine with

dx.doi.org/10.1021/jp411790v | J. Phys. Chem. A 2014, 118, 2196−2208

Table 1. Relevant Reactions for the Bromate−MESNA Reaction in Acidic Medium[a]

reaction no.	reaction	k_f; k_r
M1	$BrO_3^- + RSH + H^+ \rightarrow HBrO_2 + RSOH$	0.473
M2	$HBrO_2 + RSH \rightarrow HOBr + RSOH$	1.05×10^5
M3	$HOBr + RSH \rightarrow Br^- + H^+ + RSOH$	1.53×10^4
M4	$BrO_3^- + 2H^+ + Br^- \rightleftarrows HBrO_2 + HOBr$	2.5; 1.31×10^4
M5	$HBrO_2 + Br^- + H^+ \rightleftarrows 2HOBr$	2.01×10^9; 2.0×10^{-5}
M6	$HOBr + Br^- + H^+ \rightleftarrows Br_2 + H_2O$	8.9×10^9; 110
M7	$HOBr + RSH \rightarrow RSOH + Br^- + H^+$	1.53×10^4
M8	$HOBr + RSOH \rightarrow RSO_2H + Br^- + H^+$	3.34×10^6
M9	$HOBr + RSO_2H \rightarrow RSO_3H + Br^- + H^+$	2.06×10^4
M10	$Br_2(aq) + RSH + H_2O \rightarrow RSOH + 2Br^- + 2H^+$	1.95×10^4
M11	$Br_2(aq) + RSOH + H_2O \rightarrow RSO_2H + 2Br^- + 2H^+$	15.5
M12	$Br_2(aq) + RSO_2H + H_2O \rightarrow RSO_3H + 2Br^- + 2H^+$	1.76×10^2
M13	$RSO_2H + RSO_2H \rightleftarrows RSOH + RSO_3H$	2.24×10^4
M14	$RSOH + RSH \rightleftarrows RSSR + H_2O$	85.7; 2.20×10^4
M15	$RSSR + HOBr + H_2O \rightarrow 2RSOH + Br^- + H^+$	68.0
M16	$RSSR + Br_2 + 2H_2O \rightarrow 2RSOH + 2Br^- + 2H^+$	8.66
M17	$BrO_3^- + HBrO_2 + H^+ \rightleftarrows 2BrO_2\cdot + H_2O$	1.1×10^{-4}; approximately 0
M18	$BrO_2^\bullet + RSH \rightleftarrows RS^\bullet + HBrO_2$	1.0×10^2
M19	$2RS^\bullet \rightarrow RSSR$	1.0×10^3; 5.0×10^{-1}

[a]Forward and reverse rate constants are given, separated by a semicolon. Except for reactions involving water, the units of kinetics rate constants derived from the reactions' molecularity. Those with a single kinetics parameter were assumed to be essentially irreversible.

the C−S bond intact. Other stable sulfonic acids include trichlorosulfonic and methylaminosulfonic acid.

The combination of oxyhalogen kinetics and oxidation kinetics of the thiol group can be combined into the set of 16 reactions shown in Table 1. It is the simplest scheme that can be derived which can still adequately describe the reaction. These reactions, even if they also appear in the mechanism, above, have been relabeled M1−M16 (Table 1). They can be divided into 6 separate groups based on their function. To simplify the scheme, it is assumed that the major oxidants in the reaction mixture are HOBr and Br_2. If, as is known, that reaction M5 is rapid, then no loss in accuracy with respect to the description of the reaction occurs if one ignores $HBrO_2$ as a viable oxidant, though one would expect it to contribute to the oxidation.

(a) Initiation Reactions: M1−M3. In the absence of adequate amounts of bromide in reaction mixture, the three initial set of reactions produce enough bromide to catalyze the rest of the reaction. The bromide produced in reaction M3 can then be used in M4 to start the well-known cascade of oxybromine kinetics with second order dependence in acid and first order in bromate. In reactions with added bromide, reactions M1 − M3 can be removed with no loss in accuracy of the proposed mechanism. Bromide role is only to catalyze the reaction. As the reaction proceeds, it is produced autocatalytically (reaction R11).

(b) Standard Oxybromine Reactions: M4−M6. This is a well-known series of reactions which have been studied extensively in the analysis of the Belousov−Zhabotinsky reaction.[35] Bromate, itself is quite inert, and has to be primed through reaction M4 to generate the reactive oxidizing species; $HBrO_2$ and HOBr. Reaction M6 was studied by temperature-jump spectrophotometry and favors aqueous bromine in the strongly acidic environment utilized for this study.[50]

(c) Oxidation by HOBr: Reactions M7−M9. This is a cascade of oxidations of MESNA, through its two intermediates, by HOBr. [Note that M3 has been deliberately repeated as M7 so as to exhaust the oxidation reactions of HOBr in this section]. Oxidation by HOBr is through an oxygen atom transfer and is considered to be quite rapid. Figures 3a and 4a suggest the presence of a stable intermediate and the ESI−MS data unequivocally establishes this as the *S*-oxide. Hence the rate of oxidation of the *S*-oxide will be slower than the rates for the thiol and for the sulfinic acid.

(d) Oxidation by Aqueous Bromine: M10−M12. In this acidic environment, reaction M6 suggests formation of Br_2 will be strongly favored over HOBr, and thus the bulk of the oxidation should be borne by Br_2. Thus, reaction M10 is essentially diffusion-controlled with reaction M11 slower.

(e) Disproportionation Reaction: M13. Reaction M13 is essential. The spectrum in Figure 6b shows that, despite having enough oxidizing power for a 4-electron oxidation of the sulfur center to the sulfinic acid, the system prefers to disproportionate into a 2-electron oxidation and a 6-electron oxidation. There is never a viable accumulation of the sulfinic acid. The sulfonic acid can only be formed through the sulfinic acid which rapidly disproportionates.

(f) Possible Dimer Formation and Reaction: M14−M16. The spectrum in Figure 6a shows a low-level formation of the dimer. One viable route for formation of a dimer

dx.doi.org/10.1021/jp411790v | J. Phys. Chem. A 2014, 118, 2196−2208

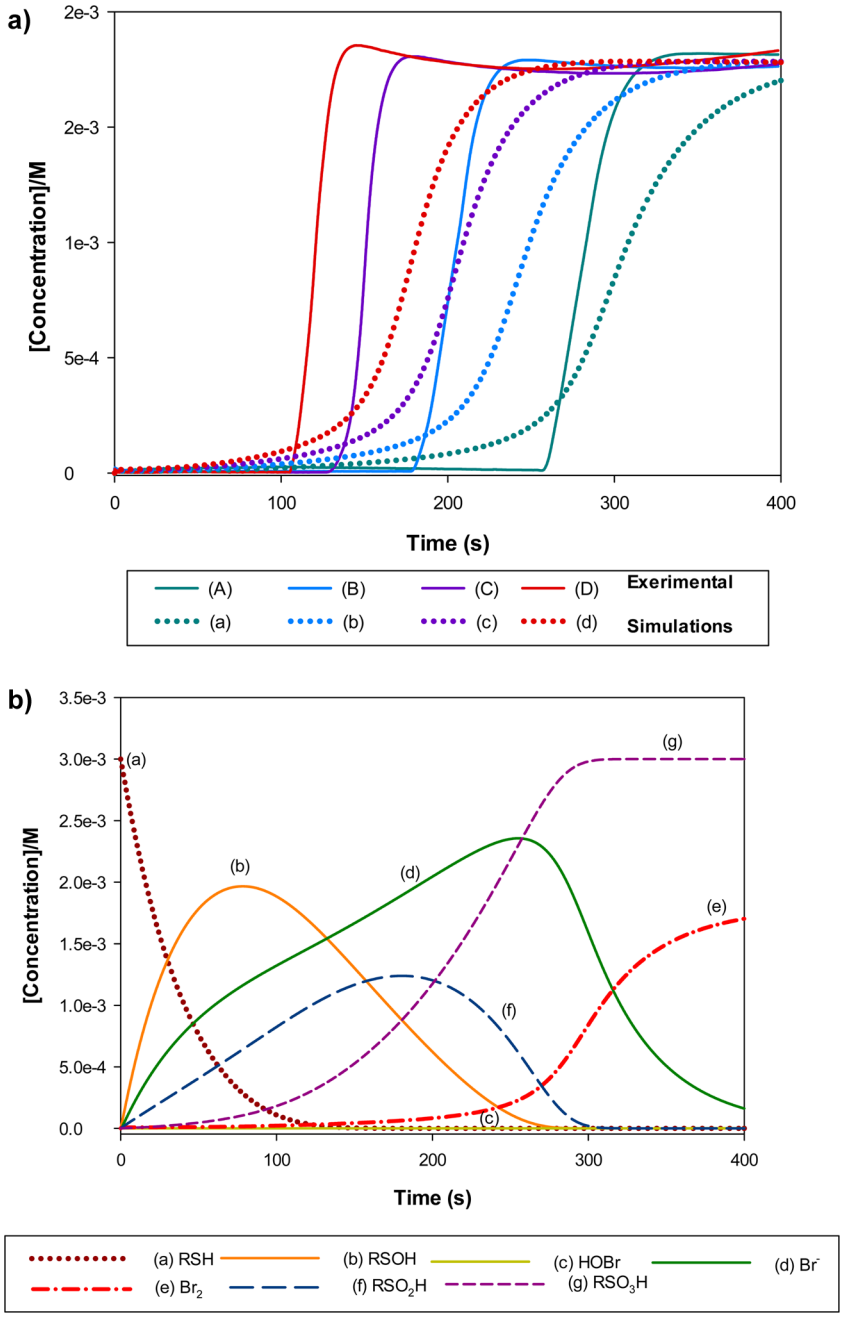

Figure 8. (a) Modeling the experimental data shown in Figure 3a, (bromate dependence). Interference from tribromide precludes a correct prediction of the rate of increase in absorbance after the induction period. As expected, the model always underestimates. The final bromine concentrations and their attainment always coincide with experiments. (b) Simulations of the intermediate species (apart from bromine) which could not be experimentally determined. No sigmoidal kinetics is observed in the consumption of MESNA, suggesting the dominance of the 2-electron oxidation pathway. The *S*-oxide coexists with bromine since it is relatively stable and its further oxidation relatively slower.

(apart from through free radicals, *vide infra*) is via a reversible condensation-type reaction between the *S*-oxide (sulfenic acid) and the unreacted thiol (M14). The dimer can be consumed via the reverse reaction of M13 in the presence of excess oxidant with further oxidation of the *S*-oxide and the thiol by HOBr and Br_2(aq). These oxidants are so powerful that they are capable of oxidizing the dimer directly (reactions M15 and M16).

(g) Contributions from Free Radicals. Figure 7 shows the formation of free radicals. The hyperfine splitting of the ESR and the 1:1:1 splitting of the peaks does not implicate the well-known hydroxyl radicals nor the superoxide radicals whose DMPO adduct spectra are well-known. Since the radical intensity is mediated by MESNA, it suggests that these are thiyl radicals and are not derived from bromine dioxide. These radicals are deactivated through the formation of the dimeric species which are evident in the spectra a and b in Figure 6. Dimer formation is also through reactions such as M14. Both mechanisms operate simultaneously because disproportionation reactions, such as those responsible for the products in spectrum b in Figure 6 can only occur through sulfur oxo-acid formations (part f, above), while Figure 7 clearly shows radical formation.

dx.doi.org/10.1021/jp411790v | J. Phys. Chem. A 2014, 118, 2196−2208

Computer Simulations. The mechanism shown in Table 1 was modeled through the SIMKINE software designed and developed by Jonnalagadda.[51,52] Reactions involving radicals, M17−M19, were not utilized for this model since their inclusion did not improve the quality of the fit. Well-known literature values were utilized and fixed for reactions M4−M6. The kinetics constant for reaction M10 was derived in this study and also fixed. The rest were optimized for best fit through a subroutine imbedded in the SIMKINE software program,[53] subject to some constraints: $k_{M10} > k_{M11} < k_{M12}$. This constraint was from the experimental observation that the *S*-oxide had a special stability associated with it. One reaction not included in the table but relevant in excess bromate environments involved the formation of tribromide:

$$Br_2(aq) + Br^- \rightleftarrows Br_3^-(aq); \quad K_{eq} = 17 \qquad \text{(R17)}$$

Without a mass balance relationship that links all bromine species (both bromine and bromide are continuously produced and consumed, with bromate as a virtual inexhaustible source of bromine), the system ends up with two equations while having three unknowns. Apart from a dynamic iterative procedure at each time interval, concentrations of bromine and tribromide could never be obtained analytically and unambiguously. While absorptivity of bromine at 390 nm is 142 M^{-1} cm^{-1}, that of tribromide is 1006 M^{-1} cm^{-1} at the same wavelength.[54] Experimental data are based on bromine absorbance, indicating that the model will always underestimate absorbance readings in environments containing bromine and bromide due to equilibrium R17 which produces a higher-absorbing species. Figure 8a shows the superimposition of experimental and simulated curves. As expected, the model shows a much slower increase in absorbance after the induction period because the model utilizes only bromine absorbances, while the experimental traces result from both bromine and tribromide absorbances. Figure 8b is a plot of the simulations of all those intermediate species which we could not experimental access. Trace e of bromine is inserted for comparison. There are four features of Figure 8b that are relevant: (a) bromide concentrations rise to a maximum just before the end of the induction period, thus delivering a large ratio of tribromide to bromine at the start of the reaction, giving the very sharp absorbance increase that is experimentally observed. (b) the *S*-oxide is very stable and rises to very high transient concentrations. Thus, when the induction period ends, although the parent thiol would have been depleted, there will still be substantial concentrations of the S-Oxide. This, then, explains what appears to be olligooscilatory behavior in bromine concentrations with a transient peak after the induction period. (c) HOBr, as expected, never rises to any substantial levels through the whole reaction. It is too reactive. (d) There is no sigmoidal decay in the rate of depletion of MESNA (trace a). This is important. If the free radical route was dominant, then $HBrO_2$ will be the autocatalytic species and classic sigmoidal autocatalytic kinetics would be observed.[32,55] It would strengthen, then, the argument that the 2-electron sulfur oxo acid route is dominant, and dimer formation mainly through reaction M14.

CONCLUSION

This short kinetics study has shown that MESNA can be oxidatively bioactivated in the physiological environment; though not as rapidly and as quantitatively shown in this study. Oxychlorine and oxybromine species exist in the physiological environment as a direct result accumulation of reactive oxygen species such as hydrogen peroxide. Superoxide and peroxides, as well, can oxidize MESNA. As a coinjectant with most anticancer drugs;[8] it is important to examine the metabolites it might generate and their possible effect in the physiological environment. This study shows that MESNA might act as an antioxidant and would moderate reactive oxygen species toxicities. A similar compound, taurine, is also known to moderate reactive oxygen species toxicity, but through the formation *N*-bromo- and *N*-chloro-derivatives.[56−59] The noncleavage of the C−S bond is important: the cleavage of the C−S bond before the oxidative saturation to the +6 oxidation state is known to initiate a cascade of genotoxic reactive oxygen species that are known to cause DNA damage.[44]

AUTHOR INFORMATION

Corresponding Author

*(R.H.S.) E-mail: rsimoyi@pdx.edu.

Notes

The authors declare no competing financial interest.

ACKNOWLEDGMENTS

This work was supported by Research Grant Number CHE 1056366 from the National Science Foundation and a Research Professorship allocation awarded to R.H.S. from the University of KwaZulu-Natal.

REFERENCES

(1) Sahni, V.; Choudhury, D.; Ahmed, Z. Chemotherapy-Associated Renal Dysfunction. *Nat. Rev. Nephrol.* **2009**, *5*, 450−462.
(2) Hanigan, M. H.; Townsend, D. M.; Cooper, A. J. Metabolism of Cisplatin to a Nephrotoxin. *Toxicology* **2009**, *257*, 174−175.
(3) Negishi, K.; Noiri, E.; Doi, K.; Maeda-Mamiya, R.; Sugaya, T.; Portilla, D.; Fujita, T. Monitoring of Urinary L-Type Fatty Acid-Binding Protein Predicts Histological Severity of Acute Kidney Injury. *Am. J. Pathol.* **2009**, *174*, 1154−1159.
(4) Pectasides, D.; Pectasides, E.; Papaxoinis, G.; Xiros, N.; Kamposioras, K.; Tountas, N.; Economopoulos, T. Methotrexate, Paclitaxel, Ifosfamide, and Cisplatin in Poor-Risk Nonseminomatous Germ Cell Tumors. *Urol. Oncol.* **2010**, *28*, 617−623.
(5) Links, M.; Lewis, C. Chemoprotectants - A Review of Their Clinical Pharmacology and Therapeutic Efficacy. *Drugs* **1999**, *57*, 293−308.
(6) Dyson, P. J.; Sava, G. Metal-Based Antitumour Drugs in the Post Genomic Era. *Dalton Trans.* **2006**, 1929−1933.
(7) de Jonge, M. J. A.; Verweij, J. Renal Toxicities of Chemotherapy. *Semin. Oncol.* **2006**, *33*, 68−73.
(8) Ludwig, U.; Riedel, M. K.; Backes, M.; Imhof, A.; Muche, R.; Keller, F. MESNA (Sodium 2-Mercaptoethanesulfonate) for Prevention of Contrast Medium-Induced Nephrotoxicity. *Clin. Nephrol.* **2011**, *75*, 302−308.
(9) Miller, R. P.; Tadagavadi, R. K.; Ramesh, G.; Reeves, W. B. Mechanisms of Cisplatin Nephrotoxicity. *Toxins* **2010**, *2*, 2490−2518.
(10) Patel, J. M. Metabolism and Pulmonary Toxicity of Cyclophosphamide. *Pharmacol. Ther.* **1990**, *47*, 137−146.
(11) Nicolao, P.; Giometto, B. Neurological Toxicity of Ifosfamide. *Oncology* **2003**, *65*, 11−16.
(12) Brock, N.; Pohl, J.; Stekar, J.; Scheef, W. Studies on the Urotoxicity of Oxazaphosphorine Cytostatics and Its Prevention 0.3. Profile of Action of Sodium 2-Mercaptoethane Sulfonate (Mesna). *Eur. J. Cancer Clin. Oncol.* **1982**, *18*, 1377−&.
(13) Scheef, W.; Klein, H. O.; Brock, N.; Burkert, H.; Gunther, U.; Hoeferjanker, H.; Mitrenga, D.; Schnitker, J.; Voigtmann, R. Controlled Clinical Studies With An Antidote Against the Urotoxicity

of Oxazaphosphorines - Preliminary-Results. *Cancer Treat. Rep.* **1979**, *63*, 501−505.
(14) Katz, A.; Epelman, S.; Anelli, A.; Gorender, E. F.; Cruz, S. M.; Oliveira, R. M.; Marques, L. A. A Prospective Randomized Evaluation of Three Schedules of Mesna Administration in Patients Receiving an Ifosfamide-Containing Chemotherapy Regimen: Sustained Efficiency and Simplified Administration. *J. Cancer Res. Clin. Oncol.* **1995**, *121*, 128−131.
(15) Park, S. B.; Howald, W. N.; Cashman, J. R. S-Oxidative Cleavage of Farnesylcysteine and Farnesylcysteine Methyl Ester by the Flavin-Containing Monooxygenase. *Chem. Res. Toxicol.* **1994**, *7*, 191−198.
(16) Del Corso, A.; Cappiello, M.; Mura, U. Thiol Dependent Oxidation of Enzymes: the Last Chance Against Oxidative Stress. *Int. J. Biochem.* **1994**, *26*, 745−750.
(17) Organisciak, D. T.; Darrow, R. M.; Jiang, Y. I.; Marak, G. E.; Blanks, J. C. Protection by Dimethylthiourea Against Retinal Light Damage in Rats. *Invest. Ophthalmol. Visual Sci.* **1992**, *33*, 1599−1609.
(18) Chinake, C. R.; Simoyi, R. H. New Experimental-Data on the Chlorite-Thiourea Reaction. *J. Phys. Chem.* **1993**, *97*, 11569−11570.
(19) Ziegler, D. M. Recent Studies on the Structure and Function of Multisubstrate Flavin-Containing Monooxygenases. *Annu. Rev. Pharmacol. Toxicol.* **1993**, *33*, 179−199.
(20) Thomas, E. L.; Grisham, M. B.; Jefferson, M. M. Myeloperoxidase-Dependent Effect of Amines on Functions of Isolated Neutrophils. *J. Clin. Invest* **1983**, *72*, 441−454.
(21) Thomas, E. L.; Bozeman, P. M.; Jefferson, M. M.; King, C. C. Oxidation of Bromide by the Human Leukocyte Enzymes Myeloperoxidase and Eosinophil Peroxidase. Formation of Bromamines. *J. Biol. Chem.* **1995**, *270*, 2906−2913.
(22) Jesaitis, A. J.; Dratz, E. A. *The Molecular Basis of Oxidative Damage by Leukocytes*; CRC Press: Boca Raton, FL, 1992.
(23) Thomas, E. L.; Grisham, M. B.; Melton, D. F.; Jefferson, M. M. Evidence for a Role of Taurine in the in Vitro Oxidative Toxicity of Neutrophils Toward Erythrocytes. *J. Biol. Chem.* **1985**, *260*, 3321−3329.
(24) Kapungu, G. P.; Rukweza, G.; Tran, T.; Mbiya, W.; Adigun, R.; Ndungu, P.; Martincigh, B.; Simoyi, R. H. Oxyhalogen-Sulfur Chemistry: Kinetics and Mechanism of Oxidation of Captopril by Acidified Bromate and Aqueous Bromine. *J. Phys. Chem. A* **2013**, *117*, 2704−2717.
(25) Darkwa, J.; Mundoma, C.; Simoyi, R. H. Reactivity and Oxidation of DL-Cysteine by Some Common Oxidants. *J. Chem. Soc., Faraday Trans.* **1998**, *94*, 1971−1978.
(26) Chigwada, T. R.; Chikwana, E.; Ruwona, T.; Olagunju, O.; Simoyi, R. H. S-Oxygenation of Thiocarbamides. 3. Nonlinear Kinetics in the Oxidation of Trimethylthiourea by Acidic Bromate. *J. Phys. Chem. A* **2007**, *111*, 11552−11561.
(27) Otoikhian, A. A.; Simoyi, R. H. Kinetics and Mechanism of Oxidation of N, N ′-Dimethylaminoiminomethanesulfinic Acid by Acidic Bromate. *J. Phys. Chem. A* **2008**, *112*, 8569−8577.
(28) Balldin, J.; Alling, C.; Gottfries, C. G.; Lindstedt, G.; Langstrom, G. Changes in Dopamine Receptor Sensitivity in Humans After Heavy Alcohol Intake. *Psychopharmacology (Berlin)* **1985**, *86*, 142−146.
(29) Sortes, C. E.; Faria, R. B. Revisiting the kinetics and mechanism of bromate-bromide reaction. *J. Braz. Chem. Soc.* **2001**, *12*, 775−779.
(30) Ajibola, R. O.; Simoyi, R. H. S-Oxygenation of Thiocarbamides IV: Kinetics of Oxidation of Tetramethylthiourea by Aqueous Bromine and Acidic Bromate. *J. Phys. Chem. A* **2011**, *115*, 2735−2744.
(31) Lopez-Cueto, G.; Ostra, M.; Ubide, C. New Way of Application of the Bromate-Bromide Mixture in Kinetic Analysis. *Anal. Chim. Acta* **2001**, *445*, 117−126.
(32) Noyes, R. M.; Field, R. J.; Thompson, R. C. Mechanism of Reaction of Bromine(V) With Weak One-Electron Reducing Agents. *J. Am. Chem. Soc.* **1971**, *93*, 7315−7316.
(33) Noyes, R. M. Chemical Oscillations and Instabilities. 39. A Generalized Mechanism for Bromate-Driven Oscillators by Bromide. *J. Am. Chem. Soc.* **1980**, *102*, 4644−4649.
(34) Szalai, I.; Oslonovitch, J.; Forsterling, H. D. Oscillations in the Bromomalonic Acid/Bromate System Catalyzed by [Ru(Phen)(3)](2+). *J. Phys. Chem. A* **2000**, *104*, 1495−1498.
(35) Mrakavova, M.; Melichercik, M.; Olexova, A.; Treindl, L. The Autocatalytic Reduction of Ferriin by Malonic Acid With Regard to the Ferroin-Catalyzed Belousov-Zhabotinsky Reaction. *Collect. Czech. Chem. Commun.* **2003**, *68*, 23−34.
(36) Sirimungkala, A.; Forsterling, H. D.; Dlask, V.; Field, R. J. Bromination Reactions Important in the Mechanism of the Belousov-Zhabotinsky System. *J. Phys. Chem. A* **1999**, *103*, 1038−1043.
(37) Petrov, V.; Scott, S. K.; Showalter, K. Excitability, Wave Reflection, and Wave Splitting in A Cubic Autocatalysis Reaction-Diffusion System. *Philos. Trans. R. Soc. London, Ser. A: Math., Phys. Eng. Sci.* **1994**, *347*, 631−642.
(38) Bala, D.; Treindl, L. Temperature and Oxygen Effect on Oscillations of the Belousov-Zhabotinsky Reaction With 2-Oxopentanedioic Acid As Substrate. *Collect. Czech. Chem. Commun.* **2000**, *65*, 1839−1847.
(39) Pullela, S. R.; Cristancho, D.; He, P.; Luo, D. W.; Hall, K. R.; Cheng, Z. D. Temperature Dependence of the Oregonator Model for the Belousov-Zhabotinsky Reaction. *Phys. Chem. Chem. Phys.* **2009**, *11*, 4236−4243.
(40) Chikwana, E.; Otoikhian, A.; Simoyi, R. H. Oxyhalogen-Sulfur Chemistry: Kinetics and Mechanism of Oxidation of Guanylthiourea by Acidified Bromatel. *J. Phys. Chem. A* **2004**, *108*, 11591−11599.
(41) Bruice, T. C.; Sayigh, A. B. The Structure of Anthraquinone-1-Sulfenic Acid (Fries' Acid) and Related Compounds. *J. Am. Chem. Soc.* **1959**, *81*, 3416−3419.
(42) Bruice, T. C.; Markiw, R. T. The Synthesis of a Disulfenic Acid. Anthraquinone-1,4-Disulfenic Acid. *J. Am. Chem. Soc.* **1957**, *79*, 3150−3154.
(43) Jenks, W. S.; Matsunaga, N.; Gordon, M. Effects of Conjugation and Aromaticity on the Sulfoxide Bond. *J. Org. Chem.* **1996**, *61*, 1275−1283.
(44) Makarov, S. V.; Mundoma, C.; Svarovsky, S. A.; Shi, X.; Gannett, P. M.; Simoyi, R. H. Reactive Oxygen Species in the Aerobic Decomposition of Sodium Hydroxymethanesulfinate. *Arch. Biochem. Biophys.* **1999**, *367*, 289−296.
(45) Chinake, C. R.; Simoyi, R. H. Kinetics and Mechanism of the Complex Bromate-Iodine Reaction. *J. Phys. Chem.* **1996**, *100*, 1643−1656.
(46) Chinake, C. R.; Mundoma, C.; Olojo, R.; Chigwada, T.; Simoyi, R. H. Oxyhalogen-Sulfur Chemistry: Kinetics and Mechanism of the Oxidation of a Bunte Salt 2-Aminoethanethiolsulfuric Acid by Chlorite. *Phys. Chem. Chem. Phys.* **2001**, *3*, 4957−4964.
(47) Chinake, C. R.; Simoyi, R. H. Oxyhalogen-Sulfur Chemistry: Oxidation of Taurine by Chlorite in Acidic Medium. *J. Phys. Chem. B* **1997**, *101*, 1207−1214.
(48) Morakinyo, M. K.; Chikwana, E.; Simoyi, R. H. Oxyhalogen-Sulfur Chemistry - Kinetics and Mechanism of the Bromate Oxidation of Cysteamine. *Can. J. Chem.—Rev. Can. Chim.* **2008**, *86*, 416−425.
(49) Mundoma, C.; Simoyi, R. H. Oxyhalogen-Sulfur Chemistry - Oxidation of 2-Aminoethanethiolsulfuric Acid by Iodate in Acidic Medium. *J. Chem. Soc., Faraday Trans.* **1997**, *93*, 1543−1550.
(50) Kustin, K.; Eigen, M. Disproportionation Kinetics of Halogens Studied by Temperature-Jump Spectrophotometry. *J. Am. Chem. Soc.* **1962**, *84*, 1355−1359.
(51) Jonnalagadda, S. B.; Pramasur, N.; Shezi, M. N. 'Simkine' for Simulation of Kinetics Involving Complex Reaction Mechanisms. *Comput. Biol. Chem.*: Elsevier: Amsterdam, 2003, *27*, 147−152.
(52) Mzolisi, N. S.; Jonnalagadda, S. B. Simkine 2 - Versatile Software for the Computation of Kinetic Profiles of Intricate Chemiscal Reaction Mechanisms. *S. Afr. J. Chem.* **2006**, *59*, 82−85.
(53) Mzolisi, N. S.; Jonnalagadda, S. B. Easy to Use Program 'Simkine 3' for Simulating Kinetics Profiles of Intricate Chemical Systems and Optimizing Predictable Rate Coefficients Therein. *Bull. Chem. Soc. Ethiop.* **2012**, *26*, 267−277.

(54) Simoyi, R. H.; Epstein, I. R. Systematic Design of Chemical Oscillators. 40. Oxidation of Thiourea by Aqueous Bromine: Autocatalysis by Bromide. *J. Phys. Chem.* **1987**, *91*, 5124−5128.
(55) Jonnalagadda, S. B.; Chinake, C.; Simoyi, R. H. Kinetics and Mechanism of the Reaction Between Thymol Blue and Bromate in Acidic Medium. *J. Chem. Soc., Faraday Trans.* **1995**, *91*, 1635−1640.
(56) Green, T. R.; Fellman, J. H.; Eicher, A. L.; Pratt, K. L. Antioxidant Role and Subcellular Location of Hypotaurine and Taurine in Human Neutrophils. *Biochim. Biophys. Acta* **1991**, *1073*, 91−97.
(57) Green, T. R.; Fellman, J. H.; Eicher, A. L. Myeloperoxidase Oxidation of Sulfur-Centered and Benzoic Acid Hydroxyl Radical Scavengers. *FEBS Lett.* **1985**, *192*, 33−36.
(58) Kearns, S.; Dawson, R., Jr. Cytoprotective Effect of Taurine Against Hypochlorous Acid Toxicity to PC12 Cells. *Adv. Exp. Med. Biol.* **2000**, *483*, 563−570.
(59) Learn, D. B.; Fried, V. A.; Thomas, E. L. Taurine and Hypotaurine Content of Human Leukocytes. *J. Leukocyte Biol.* **1990**, *48*, 174−182.